

Longitudinal and Transverse Parton Momentum Distributions for Hadrons within Relativistic Constituent Quark Models

T. Frederico*, E.Pace[†], B.Pasquini** and G. Salmè[‡]

**Dep. de Física, Instituto Tecnológico de Aeronáutica, 12.228-900 São José dos Campos, São Paulo, Brazil*

[†]*Dipartimento di Fisica, Università degli Studi di Roma "Tor Vergata" and Istituto Nazionale di Fisica Nucleare, Sezione Tor Vergata, Via della Ricerca Scientifica 1, 00133 Roma, Italy*

***Dipartimento di Fisica Nucleare e Teorica, Università degli Studi di Pavia and Istituto Nazionale di Fisica Nucleare, Sezione di Pavia, Pavia, Italy*

[‡]*Istituto Nazionale di Fisica Nucleare, Sezione di Roma, P.le A. Moro 2, 00185 Roma, Italy*

Abstract. Longitudinal and transverse parton distributions for pion and nucleon are calculated from hadron vertexes obtained by a study of form factors within relativistic quark models. The relevance of the one-gluon-exchange dominance at short range for the behavior of the form factors at large momentum transfer and of the parton distributions at the end points is stressed.

Keywords: hadron, parton distributions

PACS: 12.39.Ki, 11.10.St, 13.40.-f, 14.40.Aq

INTRODUCTION

A detailed description of hadron structure can be accessed through the generalized parton distributions (GPD's) (see, e.g., Refs. [1, 2, 3]). We determine hadron vertex functions by a study of electromagnetic (em) form factors (ff) in the spacelike (SL) region within constituent quark models, and then we use the vertex functions to evaluate the GPD's.

In this contribution we shortly review : (i) our results for the unpolarized GPD's of the pion within covariant and light-front (LF) models [4]; and (ii) our preliminary results for the unpolarized longitudinal and transverse parton momentum distributions (TMD) in the nucleon within a LF framework [5].

In order to study the GPD's in the valence region as well as in the nonvalence (NV) region, the Fock state decomposition [6] of the hadron state has to be considered : e.g. for the pion $|\pi\rangle = |q\bar{q}\rangle + |q\bar{q}q\bar{q}\rangle + |q\bar{q}g\rangle + \dots$

Isoscalar (IS) and isovector (IV) pion GPD's, $H_\pi^{0,1}(x, \xi, t)$, in the light-cone gauge are

$$H_\pi^0 = \int \frac{dz^-}{4\pi} e^{ixP^+z^-} \langle p' | \bar{\psi}_q(-\frac{z}{2}) \gamma^+ \psi_q(\frac{z}{2}) | p \rangle \Big|_{\tilde{z}=0} \quad H_\pi^1 = \int \frac{dz^-}{4\pi} e^{ixP^+z^-} \langle p' | \bar{\psi}_q(-\frac{z}{2}) \gamma^+ \tau_3 \psi_q(\frac{z}{2}) | p \rangle \Big|_{\tilde{z}=0} \quad (1)$$

where $\tilde{z} \equiv \{z^+ = z^0 + z^3, \mathbf{z}_\perp\}$, and $\psi_q(z)$ is the quark field isodoublet, while $P = \frac{1}{2}(p' + p)$, $\Delta = p' - p$, $x = k^+/P^+$, $\xi = -(p'^+ - p^+)/2P^+$, $t = \Delta^2$, with k is the average momentum of the active quark, i.e. the one that interacts with the photon (see Fig. 1). The variable x allows one to single out (i) the valence region (DGLAP [7]), for $1 \geq x \geq |\xi|$

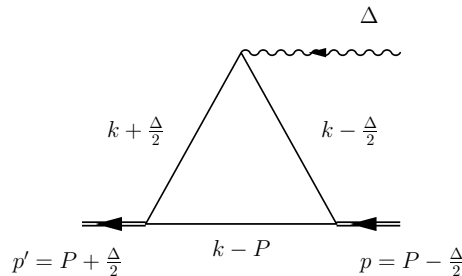


FIGURE 1. Diagrammatic representation of the pion GPD, with four momentum definitions (after Ref. [4]).

and $-|\xi| \geq x \geq -1$, diagonal in the Fock space; and (ii) the nonvalence region (ERBL [8]), for $|\xi| > x > -|\xi|$, non diagonal in the Fock space. Three pion models are used :

An analytic covariant pion model with symmetric regulators and a bare photon vertex. We use a pion Bethe-Salpeter amplitude (BSA) with a γ^5 coupling [9] and a constituent quark (CQ) mass $m = 220$ MeV. Two covariant symmetric forms for the momentum dependent part, $\Lambda(k - P, p)$, of the BSA are considered: i) a sum form, and ii) a product form, which depend on a parameter chosen to fit the pion decay constant f_π in each model. The u -quark GPD in the pion, $H^u(x, \xi, t) = H_\pi^{I=0} + H_\pi^{I=1}$, is given in *impulse approximation* by

$$H^u(x, \xi, t) = -i N_c 2 \frac{m^2}{f_\pi^2} \int \frac{d^4 k}{2(2\pi)^4} \delta(P^+ x - k^+) V^+ \Lambda(k - P, p') \Lambda(k - P, p) \quad , \quad (2)$$

where the δ function imposes the correct support, $-|\xi| \leq x \leq 1$, for the active quark, $N_c = 3$ is the number of colors, $S(k)$ the free quark propagator and $V^+ = Tr \{ S(k - P) \gamma^5 S(k + \Delta/2) \gamma^+ S(k - \Delta/2) \gamma^5 \}$. We adopt a Breit frame with $\Delta^+ = -\Delta^- \geq 0$. Then in this model the whole kinematical range $-1 \leq \xi \leq 1$ can be explored.

Mandelstam-inspired pion light-front model. We extend to GPD's [4] the model [10] for the pion ff, based on the covariant Mandelstam formula for the current [11], with a microscopic Vector Meson (VM) dominance dressing for the photon vertex. The expression of Eq. (2) for H^u holds, but the bare quark-photon vertex, γ^+ , is replaced by the VM dominance (VMD) vertex of [10]. In the k^- integration only the propagators poles are considered, i.e. the BSA analytic structure is disregarded in i) the pion state and ii) the photon vertex. The dynamical inputs are the pion and VM LF wave functions (wf's). For the tridimensional reduction of the n -th VM BSA in the valence sector, $0 < k^+ < P_n^+$, we take the eigenfunction of a relativistic mass operator [12], normalized to the probability of the valence Fock state [10]. For the pion in the valence sector the eigenfunction of the mass operator [12] is used, while for the *NV pion vertex*, a constant is assumed [13]. All of the parameters of [10] are used, but for the CQ mass $m = 200$ MeV, instead of $m = 265$ MeV. A parameter, $w = -1$, which modulates the relative weights of our two instantaneous contributions is used to fit the pion ff. For this model we take the Breit frame where $\Delta_\perp = 0$, and assume $m_\pi = 0$ (see Ref. [10]). Then $\xi = -1$ and only the NV region contributes.

Light-front Hamiltonian dynamics model. In the light-front Hamiltonian dynamics (LFHD) model [14] the Drell-Yan $\Delta^+ = 0$ reference frame is adopted and then the variable x becomes the longitudinal momentum fraction x_q , since $\xi = 0$ for any t . Within the LFHD model the pion LF wave function is

$$\Psi_\pi(x, \kappa_\perp; \lambda_q, \lambda_{\bar{q}}) = \psi_\pi(x, \kappa_\perp) \sum_{\mu_q, \mu_{\bar{q}}} (\frac{1}{2} \mu_q \frac{1}{2} \mu_{\bar{q}} |00\rangle) D_{\mu_q \lambda_q}^{1/2*} [R(\kappa)] D_{\mu_{\bar{q}} \lambda_{\bar{q}}}^{1/2*} [R(-\kappa)] \quad , \quad (3)$$

with λ_i ($i = q, \bar{q}$) the spin projections, $\kappa \equiv \{ \kappa_\perp, \kappa_z \}$, $\kappa_z = M_0(x, \kappa_\perp) (x - \frac{1}{2})$ and $M_0(x, \kappa_\perp)$ the pion free mass. The Melosh rotation $D_{\lambda, \mu}^{1/2} [R(\kappa)] = \langle \lambda | R(\kappa) | \mu \rangle$ converts the instant-form spins into LF spins and ensure the rotational covariance. For the momentum component of the pion wf we use a Gaussian form. The CQ mass $m = 250$ MeV and a parameter in the exponent are adjusted to fit f_π and the pion charge radius [4]. In this model the pion GPD $H^u(x, \xi = 0, t)$ in the range $0 \leq x \leq 1$ is given by a diagonal contribution with $n = 2$ constituents

$$H^u = \sum_{\{\lambda_i\}} \int \frac{d\kappa_\perp}{2(2\pi)^3} \Psi_\pi^*(x, \kappa'_\perp; \{\lambda_i\}) \Psi_\pi(x, \kappa_\perp; \{\lambda_i\}) \quad . \quad (4)$$

Initial and final transverse components of active quark momenta in the intrinsic frame are related by $\kappa'_\perp = \kappa_\perp + (1 - x) \Delta_\perp$. Then at large $|t|$, i.e. at large $|\Delta_\perp|$, $H^u(x, \xi = 0, t)$ is expected to be non vanishing only for $x \sim 1$.

PION LONGITUDINAL AND TRANSVERSE MOMENTUM DISTRIBUTIONS

At $\xi = 0$ one has $x = x_q$ and for $t = 0$ one gets from H^u the longitudinal momentum distribution

$$u(x) = H^u(x, 0, 0) = 2 H_\pi^{I=1}(x, 0, 0) = \int d\mathbf{k}_\perp f_1(x, k_\perp) \quad (x \geq 0) \quad , \quad (5)$$

where $f_1(x, k_\perp)$ is the TMD. The $u(x)$ distributions for our models are compared in Fig. 2. The covariant sum-form model is unable to give a vanishing value for $u(x)$ at the end points, while the product-form model describes both the

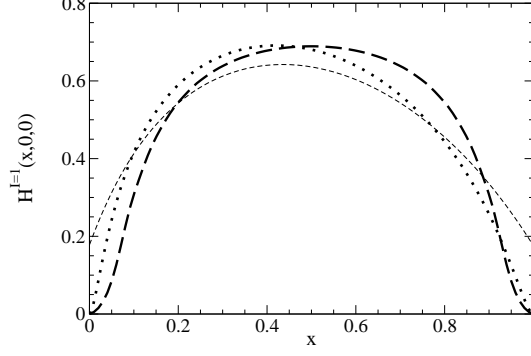


FIGURE 2. Thin dashed line: covariant model with the sum-form BSA. Dotted line: covariant model with the product-form BSA. Thick dashed line: LFHD model (after Ref. [4]).

ff tail and the end-point fall-off of the parton distribution [4]. Indeed, the product-form model has a k_{\perp}^4 fall-off of the BSA, compatible with a BSA kernel dominated by the one-gluon-exchange (OGE) and faster than the k_{\perp}^2 decay of the sum-form model, and both at $-t \rightarrow \infty$ and at $x \rightarrow 0$ or at $x \rightarrow 1$ the high momentum part of the pion state is probed.

At $|\xi| = 1$ and at $\xi = 0$ the covariant product-form model exhibits the same general behavior of the other models and for all of the considered models at high t a maximum of GPD's around $x \sim 1$ occurs [4]. This last fact has a simple kinematical explanation at $\xi = 0$. At $\xi = -1$, where only the $q\bar{q}$ pair production contributes, one has $x = 2k^+/\Delta^+$, while large $|t|$ values mean large $\Delta^+ = \Delta_z \approx 2k_{zq}$, and $2k^+ = k_q^+ - k_{\bar{q}}^+ \sim 2E_q = 2\sqrt{m^2 + \mathbf{k}^2}$, since each quark in the pair is almost on its mass shell. Then $x \sim E_q/k_{zq} \rightarrow 1$. As noticed in [4], also at $|\xi| = x$ the maximum of GPD as $-t \rightarrow \infty$ moves from $x \sim 0.5$ towards $x = 1$. The GPD at $|\xi| = x$ allows one to explore the transition from the valence to the NV region and this kinematical regime should be relevant to study single spin asymmetry [2].

NUCLEON PARTON MOMENTUM DISTRIBUTIONS

We describe the quark-nucleon vertex function through a BSA, with a Dirac structure suggested by an effective Lagrangian [15], and adopt a Breit reference frame where $\mathbf{q}_{\perp} = 0$ and $q^+ = |q^2|^{1/2}$. Our CQ mass is $m = m_u = m_d = 200$ MeV. The current in the SL region is approximated *microscopically* by the Mandelstam formula [11]

$$\langle \sigma', P'_N | j^{\mu} | P_N, \sigma \rangle = 3 N_c \int \frac{d^4 k_1}{(2\pi)^4} \int \frac{d^4 k_2}{(2\pi)^4} \sum \left\{ \bar{\Phi}'_N(k_1, k_2, k'_3, P'_N) S^{-1}(k_1) S^{-1}(k_2) \mathcal{J}^{\mu}(k_3, q) \Phi_N^{\sigma}(k_1, k_2, k_3, P_N) \right\} \quad (6)$$

where $k'_3 = k_3 + q$, $\mathcal{J}^{\mu}(k_3, q)$ is the quark-photon vertex, and \sum implies a sum over isospin and spinor indexes.

The Mandelstam formula is projected out by an analytic integration on k_1^- and k_2^- , taking into account only the poles of the propagators. Then the current becomes the sum of a purely valence contribution and a NV, pair-production contribution. Clearly, after the k^- integrations, the vertex functions depend only upon the LF three-momenta.

The quark-photon vertex has IS and IV contributions, $\mathcal{J}^{\mu} = \mathcal{J}_{IS}^{\mu} + \tau_z \mathcal{J}_{IV}^{\mu}$, and each term contains a purely valence contribution (in the SL region only) and a contribution corresponding to the pair production (Z-diagram). In turn the Z-diagram contribution can be decomposed in a bare term + a VMD term, viz

$$\mathcal{J}_i^{\mu}(k, q) = \mathcal{N}_i \theta(P_N^+ - k^+) \theta(k^+) \gamma^{\mu} + \theta(q^+ + k^+) \theta(-k^+) \left\{ Z_B \mathcal{N}_i \gamma^{\mu} + Z_{VM}^i \Gamma^{\mu}(k, q, i) \right\} \quad (7)$$

with $i = IS, IV$, $\mathcal{N}_{IS} = 1/6$ and $\mathcal{N}_{IV} = 1/2$. The constants Z_B and Z_{VM}^i are unknown weights to be extracted from the phenomenological analysis of the experimental data. According to the label i , the VMD term $\Gamma^{\mu}(k, q, i)$, which does not involve free parameters, includes IV or IS mesons. Indeed in [16] the microscopic model for the VMD, successfully used in [10] for the pion ff and based on the mass operator of Ref. [12], was extended to IS mesons.

In the valence vertexes the spectator quarks are on the k^- -shell, and the BSA momentum dependence is approximated through a nucleon wf PQCD inspired, which depend on the free mass of the three-quark system, $M_0(1, 2, 3)$,

$$\Psi_N(\tilde{k}_1, \tilde{k}_2, P_N) = P_N^+ \frac{\Lambda(k_1, k_2, k_3)|_{(k_{1on}, k_{2on}^-)}}{[m_N^2 - M_0^2(1, 2, 3)]} = P_N^+ \mathcal{N} \frac{(9 m^2)^{7/2}}{(\xi_1 \xi_2 \xi_3)^p [\beta^2 + M_0^2(1, 2, 3)]^{7/2}} \quad , \quad (8)$$

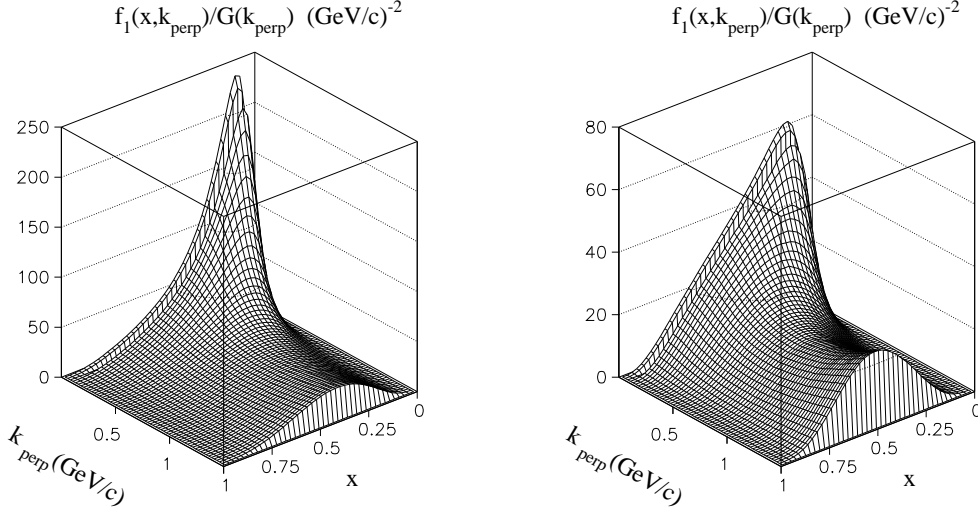


FIGURE 3. Left panel: transverse-momentum distributions for a u quark in the proton. $G(k_\perp) = (1 + k_\perp^2/m_p^2)^{-5.5}$, $m_p = 770$ MeV and $k_{perp} = k_\perp$. Right panel: the same as in the left panel, but for a d quark inside the proton (after Ref. [5]).

where $\tilde{k}_i \equiv (k_i^+, \mathbf{k}_{i\perp})$, $\xi_i = k_i^+/P_N^+$ ($i = 1, 2, 3$) and \mathcal{N} is a normalization constant. The power $7/2$ and the parameter $p = 0.13$ are chosen to have an asymptotic decrease of the triangle contribution faster than the dipole. Only the triangle diagram determines the magnetic moments, which are weakly dependent on p . Then $\beta = 0.645$ can be fixed by the magnetic moments and we obtain $\mu_p = 2.87 \pm 0.02$ ($\mu_p^{exp} = 2.793$) and $\mu_n = -1.85 \pm 0.02$ ($\mu_n^{exp} = -1.913$).

For the Z-diagram contribution, the NV vertex is needed. It can depend on the free mass, $M_0(1, 2)$, of the $(1, 2)$ quark pair and on the free mass, $M_0(N, \bar{3})$, of the (nucleon - quark $\bar{3}$) system entering the NV vertex. Then in the SL region we approximate the momentum dependence of the NV vertex $\Lambda_{NV}^{SL} = \Lambda(k_1, k_2, k_3)|_{k_{1on}, k_{3on}^-}$ by $\Lambda_{NV}^{SL} = [g_{12}]^2 [g_{N\bar{3}}]^{3/2} [k_{12}^+/P_N^+]^r [P_N^+/k_3^+]^r [P_N^+/k_3^+]^r$, with $k_{12}^+ = k_1^+ + k_2^+$ and $g_{AB} = (m_A m_B) / [\beta^2 + M_0^2(A, B)]$. The power 2 of $[g_{12}]^2$ is suggested from counting rules. The power $3/2$ of $[g_{N\bar{3}}]^{3/2}$ and the parameter $r = 0.17$ are chosen to have an asymptotic dipole behavior for the NV contribution, as suggested by the OGE dominance.

We performed a fit for the ff's of our free parameters, Z_B , Z_{VM}^i , p , r in the SL region, obtaining a $\chi^2/\text{datum} = 1.7$. The Z-diagram turns out to be essential in our reference frame with $q^+ > 0$. In particular, *the possible zero in G_E^p/G_M^p for $q^2 < 0$ is strongly related to the pair-production contribution, i.e. to higher Fock state components.*

The longitudinal distribution $q(x)$ is the limit in the forward case of the unpolarized GPD $H^q(x, \xi, t)$. For $P_N' = P_N$, both q^+ and ξ are vanishing and $x = k_3^+/P_N^+ = \xi_3$ is the fraction of the active quark longitudinal momentum. As a consequence the function $H^q(x, \xi, t)$ reduces to the longitudinal parton distribution function $q(x)$:

$$H^q(x, 0, 0) = q(x) = \int d\mathbf{k}_\perp f_1^q(x, k_\perp) = \int \frac{dz^-}{4\pi} e^{ixP^+z^-} \langle P_N | \bar{\psi}_q(-\frac{z}{2}) \gamma^+ \psi_q(\frac{z}{2}) | P_N \rangle \Big|_{z=0}, \quad (9)$$

where an average on the nucleon helicities is understood. Once all the parameters of the nucleon light-front wf $\Psi_N(\tilde{k}_1, \tilde{k}_2, P_N)$ have been determined, one can easily define the TMD of the active quark, $f_1^q(x, k_\perp)$, in terms of the LF wf and through Eq. (9) also the longitudinal distribution of the struck quark. From the isospin symmetry one has $u_p(x) = d_n(x) = u(x)$ and $d_p(x) = u_n(x) = d(x)$.

Our preliminary results for $f_1^{u(d)}(x, k_\perp)$ in the proton and for $u(x)$ and $d(x)$ are shown in Fig. 3 and in Fig. 4, respectively. It can be observed that the decay of our f_1 vs k_\perp is faster than in diquark models of the nucleon [17],

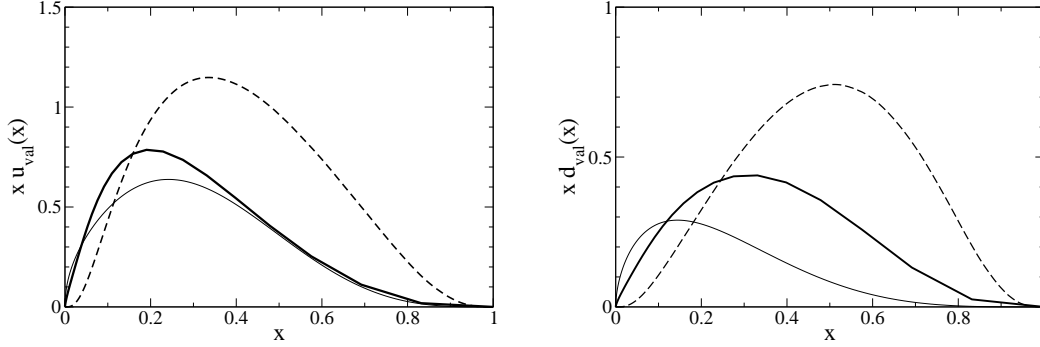


FIGURE 4. Left panel: longitudinal momentum distribution for a u quark inside the proton. Dashed lines: our preliminary results; thick solid lines: our results after evolution to $Q^2 = 1.6$ (GeV/c) 2 ; thin solid lines: CTEQ4 fit to the experimental data [19]. Right panel: the same as in the left panel, but for a d quark in the proton (after Ref. [5]).

while it is slower than in gaussian factorization models for the TMD [18]. As far as the longitudinal distributions are concerned, a reasonable agreement of our $u(x)$ with the CTEQ4 fit to the experimental data [19] can be seen in Fig. 4.

CONCLUSIONS

Microscopical models for pion and nucleon em form factors have been investigated with good results in the SL region. The Z-diagram (i.e. higher Fock state component) has been shown to be essential, in reference frames where $q^+ \neq 0$.

The analysis of the form factors allows us to get hadron vertexes that are used to evaluate the unpolarized longitudinal and transverse momentum distributions. The effects of a k_{\perp} fall-off compatible with the OGE dominance has been explored. Its role for the description of the ff tail at high $-t$ and of vanishing longitudinal parton distributions at the end points has been shown.

The covariant product-form model is able to reproduce the pion GPD's evaluated by the Mandelstam-inspired model at $|\xi| = 1$ and by the LFHD model at $\xi = 0$. Then one could argue that the product-form model contains the main ingredients for the description of the constituents inside the pion and could be applied to study experimental data.

Our next step will be the calculation of polarized longitudinal and transverse momentum distributions.

REFERENCES

1. X.-D. Ji, *J. Phys.* **G 24**, 1181 (1998); *Ann. Rev. Nucl. Part. Sci.* **54**, 413 (2004).
2. M. Diehl, *Phys. Rep.* **388**, 41 (2003).
3. S. Boffi and B. Pasquini, *Riv. Nuovo Cim.* **30**, 387 (2007).
4. T. Frederico, E. Pace, B. Pasquini, and G. Salmè, *Phys. Rev.* **D 80** (2009) 054021.
5. E. Pace, J.P.B.C. de Melo, T. Frederico, S. Pisano and G. Salmè, to be published.
6. S.J. Brodsky, H.C. Pauli, and S.S. Pinsky, *Phys. Rep.* **301** (1998) 299.
7. V. N. Gribov, L. N. Lipatov, *Sov. J. Nucl. Phys.* **15**, 438 (1972) [*Yad. Fiz.* **15** (1972) 781]; **15**, 675 (1972); G. Altarelli, G. Parisi, *Nucl. Phys.* **B 126**, 298 (1977); Yu. L. Dokshitzer, *Sov. Phys. JETP* **46**, 641 (1977).
8. A. V. Efremov, A. V. Radyushkin, *Phys. Lett.* **B 94**, 245 (1980); G. P. Lepage, S. J. Brodsky, *Phys. Rev.* **D 22**, 2157 (1980).
9. T. Frederico, G.A. Miller, *Phys. Rev.* **D 45** (1992) 4207.
10. J.P.B.C. de Melo, T. Frederico, E. Pace and G. Salmè, *Phys. Lett.* **B 581** (2004) 75; *Phys. Rev.* **D 73** (2006) 074013.
11. S. Mandelstam, *Proc. Royal Soc.* **A 233** (1956) 248.
12. T. Frederico, H.-C. Pauli and S.-G. Zhou, *Phys. Rev.* **D 66** (2002) 116011.
13. C.-R. Ji and H.-M. Choi, *Phys. Lett.* **B 513** (2001) 330.
14. P.L. Chung, F. Coester, and W.N. Polyzou, *Phys. Lett.* **B 205** (1998) 545.
15. W.R.B. de Araujo *et al.*, *Phys. Lett.* **B 478** (2000) 86; *Nucl. Phys.* **A 694** (2001) 351.
16. J.P.B.C. de Melo, T. Frederico, E. Pace, S. Pisano and G. Salmè, *Phys. Lett.* **B 671** (2009) 153.
17. R. Jacob, P.J. Mulders, J. Rodriguez, *Nucl. Phys.* **A 626** (1997) 937.
18. M. Anselmino, E. Efremov, A. Kotzinian, B. Parsamyan, *Phys. Rev.* **D 74** (2006) 074015.
19. H.L. Lai *et al.*, *Phys. Rev.* **D 51** (1995) 4763.